

PREDICTION OF SPRINGBACK IN THE FORMING OF ADVANCED HIGH  
STRENGTH STEEL: SIMULATION AND EXPERIMENTAL STUDY

NORAISHAH BINTI MOHAMAD NOOR

A thesis submitted in  
fulfillment of the requirement for the award of the  
Degree of Master of Mechanical Engineering

FACULTY OF MECHANICAL ENGINEERING AND MANUFACTURING  
UNIVERSITY TUN HUSSEIN ONN MALAYSIA

MAY 2011

## ABSTRACT

Dual Phase (DP) steel is categorized as advanced high-strength steels (AHSS) which has tensile strengths ranging from 500 to 800 MPa. DP steel is gaining popularity in automotive applications. It has higher formability than HSLA grades with similar initial yield strengths, but has much higher final part strength. With proper design strategy, Dual Phase (DP) steels offers a great advantage in terms of body weight reduction and crash performance. One of the major constraints in forming AHSS is the occurrence of high springback caused by elastic relaxation after loading, which causes ill-fitting in part assembly and geometric deviation of the intended design. This research focused on finite element (FE) simulation of the sheet forming of dual phase steel and the springback prediction. If springback could be accurately predicted, the forming die could be correctly designed to compensate springback. The material used in this study was DOCOL 800 DP manufactured by SSAB- Sweden with ultimate tensile strength of 870 MPa and thickness of 0.72mm. The plastic behavior of DP800 was presented by exponential based constitutive equation known as isotropic hardening. From tensile test, strain hardening value ( $n$ ) was 0.308 and strength coefficient ( $K$ ) was 1319.165 MP. The FE simulations were conducted for tensile test, U-channel forming and springback simulation. These simulations were carried out by using general purpose transient dynamic FE code Lsdyna. The tensile test simulation result indicated the isotropic hardening material model was suitable for DP800 behavior with standard deviation value 62.45 MPa between simulation and experiment. Meanwhile, the springback simulation using U-channel represented the deviation for BHF 10kN, 20kN, 30kN and 97kN were 0.019, 0.071, 0.341 and 0.231. Overall, the result of 20KN BHF applied indicated the minimum springback in the forming of DP800.

## ABSTRAK

Keluli Dual Phase (DP) dikategorikan sebagai *advanced high-strength steels* (AHSS) dimana, kekuatan tarikan dalam lingkungan 500 hingga 800 MPa. Keluli DP semakin popular dalam aplikasi automotif. Keluli ini mempunyai sifat mampu bentuk dan kekuatan luluh yang sama dengan gred HSLA namun kekuatan yang lebih tinggi. Dengan strategi rekabentuk yang baik, keluli DP mempunyai lebih banyak kelebihan dari segi pengurangan berat dan prestasi perlanggaran. Antara kekangan utama dalam pembentukan AHSS adalah kejadian *springback* oleh relaksasi elastik selepas pembebanan yang mana menyebabkan masalah kepada penyesuaian dalam pemasangan bahagian serta deviasi geometri yang dimaksudkan dalam rekabentuk tersebut. Kajian ini fokus kepada simulasi kaedah unsur (FE) terhitung pada lembaran logam DP dan prediktasi *springback*. Sekiranya *springback* boleh diprediktasi dengan tepat, rekabentuk *die* yang lebih baik dapat dihasilkan bagi mengimbangi *springback*. Bahan yang digunakan dalam kajian ini adalah DOCOL 800 DP dihasilkan oleh SSAB-Sweden dengan kekuatan tarik maksimum adalah 870MPa dengan ketebalan 0.72mm. Gayalaku plastik DP800 ditunjukkan dengan exponential berdasarkan *Isotropic Hardening constitutive model*. Daripada ujikaji penarikan, *strain hardening value* ( $n$ ) adalah 0.308 dan *strength coefficient* ( $K$ ) adalah 1319.165 MP. Simulasi FE dilakukan keatas ujian penarikan, pembentukan *U-channel* dan prediktasi *springback*. Simulasi ini dijalankan menggunakan kaedah umum kod *transient* dinamik FE Ls-dyna. Keputusan ujian penarikan menunjukkan model pengerasan isotropik bersesuaian dengan sifat P800 dengan piawaian diviasi sebanyak 62.45MPa diantara simulasi dan eksperimen. Manakala, untuk simulasi *springback* menunjukkan deviasi untuk BHF 10kN, 20kN, 30kN dan 97kN adalah 0.019, 0.071, 0.341 dan 0.231. Secara keseluruhan keputusan, pada nilai BHF 20kN yang dikenakan menunjukkan *springback* yang minimum dalam pembentukan DP800.

## CONTENTS

<b>TITLE</b>	<b>i</b>
<b>DECLARATION FORM</b>	<b>ii</b>
<b>DEDICATION</b>	<b>iii</b>
<b>ACKNOWLEDGEMENT</b>	<b>iv</b>
<b>ABSTRACT</b>	<b>v</b>
<b>ABSTRAK</b>	<b>vii</b>
<b>TABLE OF CONTENTS</b>	<b>viii</b>
<b>LIST OF TABLES</b>	<b>xiii</b>
<b>LIST OF FIGURES</b>	<b>xv</b>
<b>LIST OF ABBREVIATIONS</b>	<b>xx</b>
<b>LIST OF APPENDICES</b>	<b>xxi</b>
 <b>CHAPTER I</b>	
<b>INTRODUCTION</b>	
1.1 Research Background	1
1.2 Problem Statement	3
1.3 Research Aim	4
1.4 Objectives of Study	4
1.5 Scope of Study	5
1.6 Research Significances	5

## **CHAPTER II LITERATURE REVIEW**

2.1	Introduction	7
2.2	Advanced High Strength Steel	8
	2.2.1 Properties of Dual Phase	10
2.3	Sheet Metal Forming	12
	2.3.1 Sheet Metal Forming Process	13
2.4	Springback	15
	2.4.1 Basic Theory of Springback	15
	2.4.2 Springback Prediction Technique	20
2.5	Finite Element Analysis	21
	2.5.1 Application of FEM in Metal Forming	22
	2.5.2 Finite Element Software	24
2.6	Plasticity	26
	2.6.1 Tensor Stress and Tensor Strain	28
	2.6.2 Yield Criterion	28
	2.6.3 Flow Rule	30
	2.6.4 Material Constitutive Model	31
	2.6.4.1 Isotropic Hardening	32

## **CHAPTER III METHODOLOGY**

3.1	Flow Chart of Research	36
3.2	Material	38
3.3	Metallographic Examination	39
3.4	Tensile Test	42
	3.4.1 Specimen Preparation	42
	3.4.2 Tensile Test Parameters	44

	3.4.3 Tensile Testing Machine	44
3.5	Finite Element Simulation	46
	3.5.1 DYNAFORM	47
3.6	Stamping Try Out	48
	3.6.1 The Forming Setup for Experimental	49
3.3.5	3.6.2 Measurement of Experiment Output	50

## **CHAPTER IV DETERMINATION OF MATERIAL PROPERTIES**

4.1	Introduction	51
4.2	Flow Chart of Microstructure Observation	52
4.3	Metallographic Examination Results	53
	4.3.1 The Microstructure Results	53
4.4	Tensile Test Result	55
	4.4.1 Stress-Strain Curve	55
	4.4.2 Elasticity Modulus	58
	4.4.3 Elasticity Limit	60
	4.4.4 Homogenous Deformation	61
	4.4.5 Yield Strength	63
	4.4.6 Ultimate Strength	65
	4.4.7 Strain Hardening Coefficient	67
	4.4.8 Plastic Anisotropy	70
4.5	Discussion	71

## CHAPTER V FINITE ELEMENT SIMULATION

5.1	Introduction	74
5.2	Flow Chart of FE Simulation	75
5.3	Selection of Material Constitutive Model	76
5.3.1	Tensile Test Simulation	76
5.3.2	Material Model 12	77
5.3.3	Material Model 18	82
5.3.4	Material Model 24	87
5.3.5	Discussion of Tensile Test Simulation Result	93
5.4	Simulation of Deep Drawing Process	96
5.4.1	Governing Equation	96
5.4.2	Time Integration	100
5.4.3	Modeling the Geometry and Meshing	104
5.4.4	Boundary Conditions	107
5.4.5	Contact Definition	109
5.4.6	Simulation Results	109
5.5	Springback Prediction	114
5.5.1	Prediction Results	115
5.6	Verification of Simulation result	118
5.6.1	Stamping Try Out	119
5.6.2	The Forming Setup for Experiment	119
5.7	Testing Result and Discussion	120
5.8	Result and Discussion of Simulation and Stamping Comparison	122

**CHAPTER VI CONCLUSION**

6.1 Conclusion 126

6.2 Suggestion 127

**REFERENCE** 129

**APPENDIX** 132



## LIST OF TABLES

2.1	The characteristics of sheet metal forming processes	13
2.2	Basic steps of FEM application in metal forming	23
3.1	Chemical properties of DP800 provided by supplier	38
3.2	Mechanical properties of DP800 provided by supplier	38
3.3	Tensile test specimen dimension	44
3.4	Experimental parameters used	49
4.1	The young modulus for $0^\circ$ , $45^\circ$ and $90^\circ$	60
4.2	Elasticity limit of rolling direction $0^\circ$ , $45^\circ$ and $90^\circ$	61
4.3	Homogenous limit of rolling direction $0^\circ$ , $45^\circ$ and $90^\circ$	63
4.4	Yield strength values of rolling direction $0^\circ$ , $45^\circ$ and $90^\circ$	65
4.5	Ultimate strength values of rolling direction $0^\circ$ , $45^\circ$ and $90^\circ$	67
4.6	Strain hardening Coefficient values of rolling direction $0^\circ$ , $45^\circ$ and $90^\circ$	68
4.7	Strain hardening coefficient and strength coefficient obtained from logarithmic stress-strain curve	71
4.8	The value of parameters DP800	72

4.9	Examples of modified equation of power law	73
5.1	Parameter Values for Material Model 12	79
5.2	Strain and Stress Values obtained from Tensile Simulation using Material Model 12	81
5.3	Parameter Values for Material Model 18	83
5.4	Strain and Stress Values obtained from Tensile Simulation using Material Model 18	86
5.5	Parameter Values for Material Model 24	89
5.6	Strain and Stress Value obtained from Tensile Simulation using Material Model 24	92
5.7	The Comparison of Maximum Thickness Changes based on BHF applied between experimental and simulation.	123
5.8	Result comparative of experimental and simulation	124

## LIST OF FIGURES

1.1	Purpose of light weight components.	2
2.1	The schematic structure and microstructures of DP steel	8
2.2	Strength – Formability relationship for conventional HSS and Advance HSS	9
2.3	Schematic illustration of DP microstructure	10
2.4	The actual microstructure of DP steel	11
2.5	Comparison of quasi-static stress-strain behaviour of HSLA 350/450 and DP 350/600 steels	11
2.6	Schematic illustration of springback	16
2.7	The elastic unloading after removal of the loads results in the residual stresses	17
2.8	The stress distribution under bending moment and after unloading for work-hardening material	19
2.9	Details of NUMISHEET’93 benchmark	21
2.10	Measurement parameters for springback	21
2.11	Isotropic Hardening, in which the yield surface expands with plastic deformation and the corresponding uniaxial stress-strain curve	33
2.12	Stress-Strain Curve for Linear Strain Hardening	34
3.1	Methodology chart	37
3.2	Flow Chart of Microstructure Observation	39
3.3	Mounted sample	40
3.4	Hand grinder	41
3.5	Polisher	41
3.6	Tensile specimen dimensions	43

3.7	Tensile specimen	43
3.8	Angular consideration of metal sheet rolling direction	44
3.9	Universal Tensile Machine	45
3.10	Simulation flow chart	46
3.11	Components of eta/DYNAFORM solution	48
3.12	Schematic of U-channel Deep Drawing	48
3.13	Tool setup for the experiment	49
3.14	The vertical profile projector	50
4.1	Metallography flow chart	52
4.2	Docol 800DP at longitudinal direction as delivered. Nital. 1000 $\times$ .	53
4.3	Docol 800DP at longitudinal direction with 10% of tensile deformation. Nital. 1000 $\times$	53
4.4	Docol 800DP at longitudinal direction with 20% of tensile deformation. Nital. 1000 $\times$ .	53
4.5	Docol 800DP at longitudinal direction with 30% of tensile deformation. Nital. 1000 $\times$ .	53
4.6	Void found on surface of specimen with 30% of tensile deformation in SEM observation. Nital. 2000 $\times$ .	54
4.7	Stress-strain curve of DP800	56
4.8	Elastic stress-strain curve of tensile test for 0 degree rolling direction	58
4.9	Elastic stress-strain curve of tensile test for 45 degree rolling direction	59
4.10	Elastic stress-strain curve of tensile test for 90 degree rolling direction	59
4.11	Homogenous Limit of 0 degree rolling direction in Stress-Strain Curve	61
4.12	Homogenous Limit of 45 degree rolling direction	62

	in Stress-Strain Curve	
4.13	Homogenous Limit of 90 degree rolling direction in Stress-Strain Curve	62
4.14	Yield Strength Point of 0 degree rolling direction in Stress-Strain Curve	63
4.15	Yield Strength Point of 45 degree rolling direction in Stress-Strain Curve	64
4.16	Yield Strength of 90 degree rolling direction Point in Stress-Strain Curve	64
4.17	Ultimate Strength of 0 degree rolling direction Point in Stress-Strain Curve	66
4.18	Ultimate Strength of 45 degree rolling direction Point in Stress-Strain Curve	66
4.19	Ultimate Strength of 90 degree rolling direction Point in Stress-Strain Curve	77
4.20	Stress-strain of 0 degree rolling direction at plastic area in logarithmic diagram	69
4.21	Stress-strain of 45 degree rolling direction at plastic area in logarithmic diagram	69
4.22	Stress-strain of 90 degree rolling direction at plastic area in logarithmic diagram.	70
5.1	Simulation flow cart	75
5.2	Model representation of tensile sample test	77
5.3	The displacement data form tensile test simulation using Material Model Type 12	79
5.4	Considered Nodes after Deformation (M12)	80
5.5	Stress Distribution after Deformation (M12).	80
5.6	The Plastic Strain after Deformation (M12).	81
5.7	True Stress-Strain curve used in modeling the tensile specimen (nodes 1274) for M12	82

5.8	The displacement data form tensile test simulation using Material Model Type 18	84
5.9	Considered Nodes after Deformation (M18)	84
5.10	Stress Distribution after Deformation (M18)	85
5.11	The Plastic Strain after Deformation (M18).	85
5.12	True Stress-Strain curve used in modeling the tensile specimen (node 1274) for M18.	86
5.13	Rate effects may be accounted for by defining a table of curves	89
5.14	The displacement data from tensile test simulation using Material Model Type 24	90
5.15	Considered Nodes after Deformation	91
5.16	Stress Distribution after Deformation	91
5.17	The Plastic Strain after Deformation	92
5.18	True Stress-Strain curve used in modeling the tensile specimen (nodes 1274)	93
5.19	Plot true stress-true strain from modeling (M12) and from uniaxial tensile test	95
5.20	Plot true stress-true strain from modeling (M18) and from uniaxial tensile test	95
5.21	Plot true stress-true strain from modeling (M24) and from uniaxial tensile test	96
5.22	Notation	97
5.23	Tooling geometry	105
5.24	The meshing Parts	105
5.25	The diagram of parts positioning in simulation	106
5.26	Belytschko-Tsay shell element formulation	107
5.27	Parts and blank positioning before constraint and loading option	108
5.28	The constraint and loading applied	109
5.29	The changes of material thickness after forming	110

	process (BHF 10KN)	
5.30	The FLD data after forming process (BHF 10KN)	111
5.31	The changes of material thickness after forming process (BHF 20KN)	111
5.32	The FLD data after forming process (BHF 20KN)	112
5.33	The changes of material thickness after forming process (BHF 30KN)	112
5.34	The FLD data after forming process (BHF 30KN)	113
5.35	The changes of material thickness after forming process (BHF 97KN)	113
5.36	The FLD data after forming process (BHF 97KN)	114
5.37	The changes of geometry before and after springback (BHF 10KN)	115
5.38	The changes of geometry before and after springback (BHF 20KN)	116
5.39	The changes of geometry before and after springback (BHF 30KN)	117
5.40	The changes of geometry before and after springback (BHF 97KN)	118
5.41	The parameters taken account to measure springback in simulation and real U-Forming experiment	120
5.42	The usual of sample displayed by the screen of vertical profile projector	120
5.43	Example of test sample after deformation	121

## **LIST OF ABBREVIATIONS AND ACRONYMS**

FE	-	Finite Element
FEM	-	Finite Element Method
FEA	-	Finite Element Analysis
AHSS	-	Advanced High Strength Steel
HSLA	-	High Strength Low Alloy
UHSS	-	Ultimate High Strength Steel
BH	-	Bake Hardening
SMF	-	Sheet Metal Forming
ASTM	-	American Standard Testing and Material
DP	-	Dual Phase
FLD	-	Forming Limit Diagram
SIGY	-	Yield Stress
ETAN	-	Plastic Hardening Modulus
MPa	-	Mega Pascal



**LIST OF APPENDICES**

<b>APPENDIX</b>	<b>TITLE</b>	<b>PAGE</b>
A	DOCOL DP/DL MATERIAL DATASHEET	140
B	THE EXAMPLE CALCULATION FOR TENSILE TEST	143
C	ASTM (Designation E 8M-04)	
D	DYNAFORM INPUT FILE OF TENSILE TEST SIMULATION FOR M18	144
E	DYNAFORM INPUT FILE FOR FORMING SIMULATION	148
F	DYNAFORM INPUT FILE FOR SPRINGBACK SIMULATION	152
G	TENSILE TEST DATA OF EXPERIMENTS AND SIMULATIONS	155

## **CHAPTER I**

### **INTRODUCTION**

#### **1.1 Research Background**

The application of Advanced High Strength Steel (AHSS) is increasing due to the demand of light weight construction in order to improve fuel economy. Lightweight materials of AHSS such as Dual Phase steel (DP) are now used in modern automotive structure due to their best combination of metallurgical and physical properties.

Lightweight properties are crucial where mass is critical to enable the product function, such as aeronautical applications. Where masses are subject to acceleration, lightweight components can increase the product performance, e.g. allow higher revolutions with lighter crankshafts. Driving comfort and safety can be increased when unsprung masses are reduced as in a car chassis reducing masses also improves the fuel consumption. Much effort is being put into the development of lightweight components and structures in automotive applications, which can be seen in Figure. 1.1.

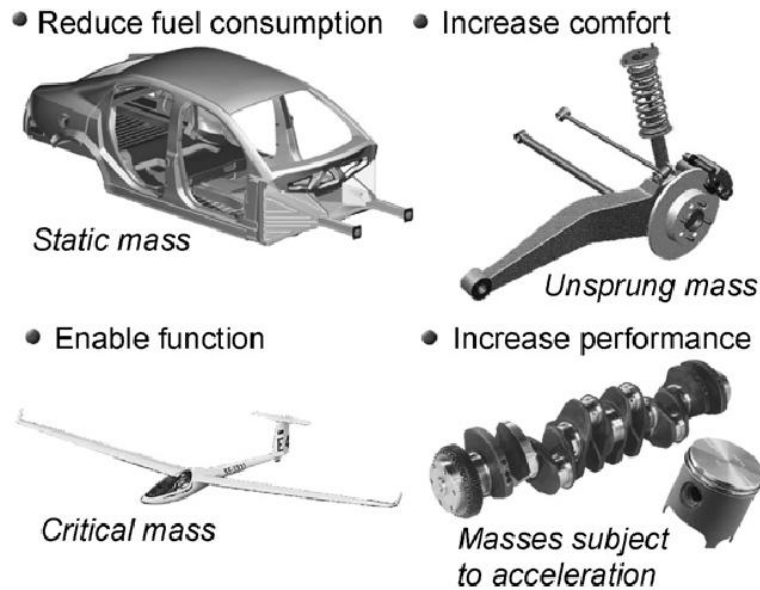


Figure 1.1: Purpose of light weight components (Jeswiet J et.al, 2008)

However, the higher the strength of a material, the worse its formability and ductility become. Thus the application of advanced high strength steel (AHSS) in automotive industry is still limited due to challenge of springback and formability. The applied force stresses the metal beyond its yield strength, causing the material to plastically deform, but not to fail. By doing so, the sheet can be bent or stretched into a variety of complex shapes. Nevertheless there will be changes of the sheet geometry after unloading process caused by elastically-driven. This process is termed as springback. The springback is not categorised as totally defect but this phenomenon causing ill fitting in joining part.

The springback deformation of sheet metal parts is a natural result of a sequence of deformation experienced in metal forming process. As the sheet metal slides over a die shoulder, it undergoes bending-unbending deformation developing cyclic bending loads on the sheet sections, and as a result an unbalanced stress distribution is developed over the thickness. (Firat M., 2007).

Springback can be predicted using Finite Element Method (FEM). The FEM is firmly accepted as a powerful general technique for the numerical solution of a variety of problems encountered in engineering. It provides more information of process parameters. Indirectly, these methods can save cost and assist to get a more accurate geometric product rather than traditional method which only depends on trial and error.

Based on FEM, important information such as the angle of springback, thickness distribution and geometry part after loading can be obtained accurately by provided the complexity of die geometry, friction conditions, absolute data of material properties etc.

Based on the prediction, the geometry and process parameters will be modified to obtain the required product shape. Efforts to springback prediction have employed both analytical and numerical approaches. According to Song N. et al.,(2004), there were some of the instances associated with this study that are conducted the analytical study by assuming that bending moment vanishes as the elastic recovery occurs and then the study is extended from Monfort G. and Bragard A.(1985) which used a cantilevered model with a non-uniform moment distribution from the contact point to the outer sheet. Then Cao J. et al.(1999) proposed a linear moment distribution in the contact area, and this model compares favorably with the experiment result of Liu Y.C, (1984). The major difficulty with analytical solution is due to the lack of understanding of the stress distribution, throughout the sheet, which limit the analytical approach is due to lack of understanding of the stress distribution throughout the sheet, which limit the analytical approach to simple geometries and deformation.

## **1.2 Problem Statement**

Finite element simulation and springback prediction on AHSS have been reported by many researchers. Liu Y.C, (1984) emphasized on process variables, which affect springback in springback in the double-bend technique. He optimized the parameters forming by using FEA program, which is ABACUS to validate with experimental based on isotropic hardening as the constitutive model. While Crisbon D J., (2003), focused on the evaluated processing parameters in addition to material parameters in relation to their overall contribution to springback using 6022-T4 aluminium alloy. She used the Taguchi method to evaluate the relative contribution of process and material parameters on springback. FEA was conducted using ANSYS implicit and compared to Barlat's 2000 anisotropic material model. U-channel forming analysis also has been study by Firat M. (2007), with emphasis on springback simulation using Ansys FEA software and

suggested that to improve the prediction is performed the simulation using implicit FE analyses based on the kinematic hardening plasticity.

However, few studies reported on springback prediction of DP using the exponential based constitutive model. Therefore, this research proposed the DP800 properties determination and Ls-dyna simulation based on exponential constitutive material model for FE simulation of the forming and springback prediction. The simple experimental of U-channel forming operation were done to validate the simulation result.

### **1.3 Research Aim**

The aim of this research is to conduct forming simulation and springback prediction of dual phase steel by using finite element simulation.

### **1.4 Objectives of Study**

The main objectives of this study are:

- i. To determine the material properties of Dual Phase steel by using the experiment data from tensile test as well as metallographic examination.
- ii. To select the suitable material constitutive models provided by Ls-dyna FE code.
- iii. To conduct FE simulation for sheet forming and predict the springback.
- iv. To validate the simulation result by comparison with U-channel forming experimental study.

## 1.5 Scope of Study

- i. Sheet forming parameters included in FE simulation were only mechanical loading namely; force and speed. Other parameters such as temperature and contact conditions are not included in the analysis.
- ii. Material sample is AHSS namely DP800 with thickness 0.72mm.
- iii. The geometry part of simple operation U-channel shape is choosing to measure springback.
- iv. Tensile test is based on Standard test method ASTM E 8M-04.
- v. The simulation is conducted by using FE code LS-dyna in which explicit time integration applied. The simulation consists of two major steps, which are loading (forming) and unloading (springback). The springback simulation use implicit time integration method.
- vi. Results obtained and taken into account is the height from the base ( $dh$ ) of the U-channel shape from FE simulation before and after springback, the strip width ( $dz$ ), main angle of the U-channel ( $\alpha$ ).

## 1.6 Research Significances

The significances of the research are as the following:

- i. The successful study on plasticity of AHSS can lead to better understanding and optimize the usage of AHSS. The knowledge and data defined for the characteristic of AHSS can be widely used to gain its best performance in forming operation and prevent failure occurrence
- ii. The result from this study can be used as a guideline for the DP800 stamping process and also can be further developed into a larger scope such as the tool and die design, springback simulation for real geometry and for steel multistep forming.
- iii. Data collected from the study can be published in journal, article or other form type as reference for other researchers or anyone who are interested in

exploring about AHSS. Particular institute, university or organization can keep result or data obtained from the study as the database for future reference in further research or data exchange.

## **CHAPTER II**

### **LITERATURE REVIEW**

#### **2.1 Introduction**

The trend for the use of advanced high strength steel in automotive industry has grown progressively in last decades. This has encouraged most researchers to study the type of steel in order to optimize weight for fuel economy and structural stiffness in safety. One of this steel is Dual Phase.

Dual phase (DP) steels commonly used in structural applications where they have replaced more conventional high strength low alloy steel (HSLA). This replacement gives a great opportunity for part weight reduction. Today's application included front and rear rails, crush cans, rocker reinforcements, back panels and door intrusion beams. Recently dual phase steels are gaining popularity in automotive closures. Dual phase steels presented higher formability than micro-alloyed steels of comparable strength.

However, the higher the strength, the worse its formability becomes. Thus the application of AHSS still limited due to challenge of springback and formability. Although, springback may not be categorized as a totally defect, this geometrical discrepancy can cause ill-fitting in part assembly and geometric deviation of the intended design.



## 2.2 Advanced High Strength Steel

Advanced high strength steels (AHSS) are hardened by phase transformation, and the microstructure may include Martensite, Bainite and retained Austenite. AHSS, including dual phase steel, TRIP and ductility combination as compared with conventional HSS and thus facilitate the energy absorption during impact and ensure safety when reducing weight according to Xiaoding Z. et al.(2007). AHSS for auto-making included hot-rolled, cold-rolled and hot dip galvanized steel, which are all strengthened by phase transformation hardening through the processing parameters, are somewhat different. Figure 2.1 indicates the schematic structure and microstructure of DP steel.

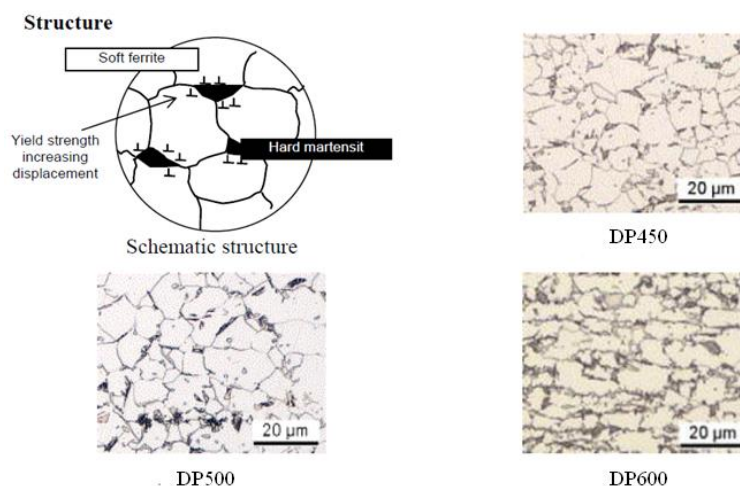


Figure 2.1: The schematic structure and microstructures of DP steel (Material Data Sheet of DP, 2005)

The principal differences between conventional high strength steel (HSS) and AHSS are due to their microstructures. AHSS gained their high-performance properties in strength and formability by incorporating multi-phase microstructures, which contain ferrite, martensite, bainite and/or retained austenite in quantities sufficient to produce unique mechanical properties in yield strength and ultimate tensile strength. Specific microstructures result from precise control of the chemistry or alloying elements. The

yield strengths of AHSS overlap the range of strengths between HSS and ultra high strength steel (UHSS) as shown in Figure 2.2.

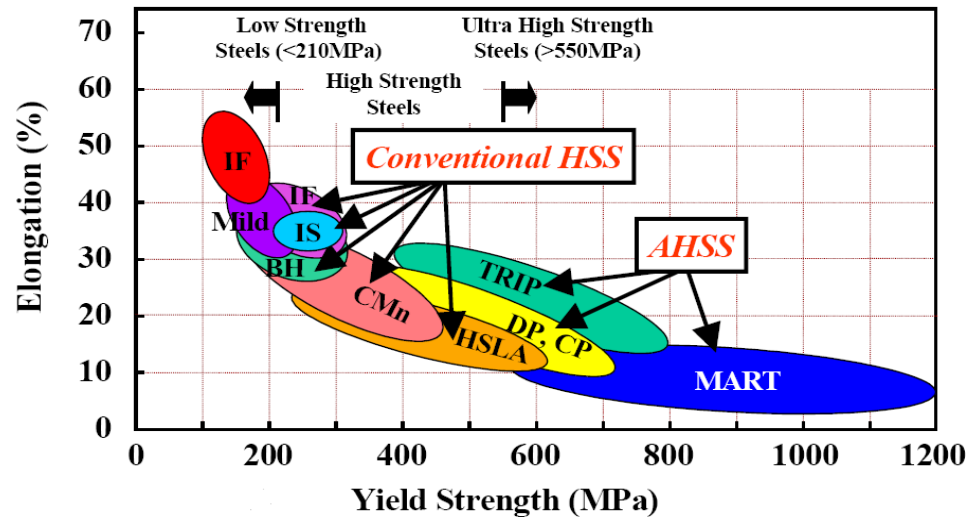


Figure 2.2: Strength – Formability relationship for conventional HSS and Advance HSS (International Iron & Steel Institute,2006).

Work and bake hardening also contributing to AHSS capabilities to provide these benefits, which can increase the material yield strength by as much as 50 percent as they undergo processing from flat sheets to complex automotive parts. The work hardening takes effect during the forming process and the bake hardening occurs as the material passes through a paint-curing process.

AHSS offered the potential for improvement in vehicle crash performance without the extra weight increase because of their excellent strength and formability combinations. Currently, two types of advanced high strength steels are being used in the automotive industry. One is the dual phase (DP) steel in which ferrite and martensite are the primary phases, and its mechanical properties are controlled by the martensite volume fraction and the ferrite grain size.

In industries, although the AHSS is good material to select as part of automotive components but the main problem of this type of steel is springback that occurred after stamping. The automotive industry places rigid constraints on final shape and dimensional tolerances. Compensating for springback becomes critical in this highly automated environment.

### 2.2.1 Properties of Dual Phase Steel

Dual Phase (DP) steel is classified as advanced high strength steels (AHSS). Generally, DP steel usually contains some alloy additions such as manganese or silicon. The strengthening effect employed in these steels is the formation of martensite or bainite in the ferrite matrix. DP steel consists of a ferritic matrix containing a hard martensitic second phase in the form of islands. (Kenneth G. B and Michael K.B,1999)

This phenomenon involves the formation of strain-induced martensite by deformation of metastable austenite and leads to the increase of strength, ductility, and toughness of the steel. DP is alloyed to control the amount and transformation of intercritically formed austenite. The carbon contents in these steels typically range from 0.05 to 0.2 wt-% C, and the manganese content may be up to 1.5 wt-%.

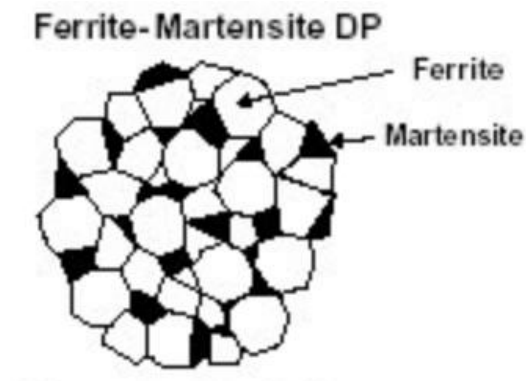


Figure 2.3: Schematic illustration of DP microstructure ([www.steel.org](http://www.steel.org))

The volume fraction of hard second phases determines its strength, and the soft ferrite phase gives this steel excellent ductility. In some example, hot rolled DP steels can have a microstructure also containing significant quantities of bainite which is required to enhance its capability to resist stretching on a blanked edge. If DP steel is deformed, strain is concentrated in the lower-strength ferrite phase surrounding the islands of martensite. This creates the unique high work-hardening rate. The work hardening rate plus excellent elongation gave DP steels much higher ultimate tensile strength than conventional steels of similar yield strength (Sugimoto KI et.al,1992).

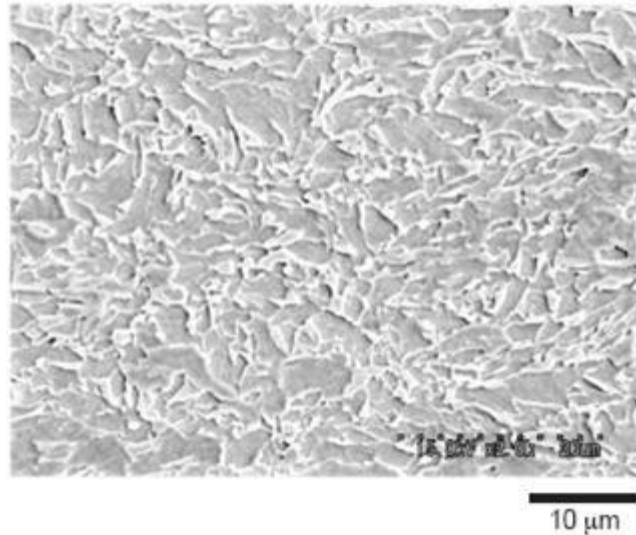


Figure 2.4: The actual microstructure of DP steel (<http://www.keytometals.com>)

Figure 2.3 and Figure 2.4 displays the micro-structure of a DP ferrite + martensite steel with 350 MPa yield strength and 600 MPa. The soft ferrite phase is generally continuous, giving these steels excellent ductility. When these steels deform, the strain is concentrated in the lower strength ferrite phase, creating the unique high work hardening rate exhibited by these steels.

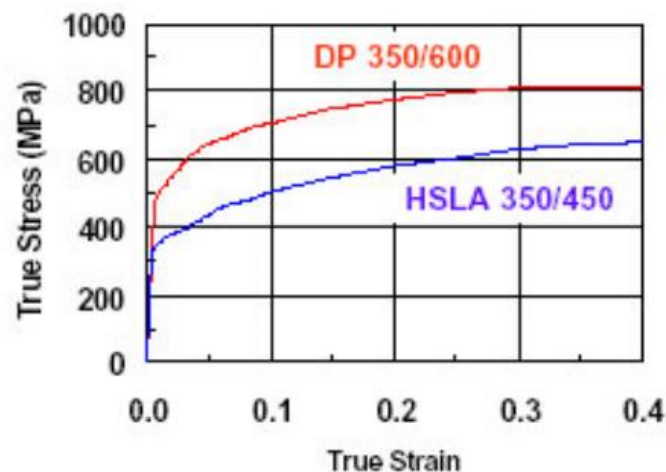


Figure 2.5: Comparison of quasi-static stress-strain behavior of HSLA 350/450 and DP 350/600 steels ([www.steels.org](http://www.steels.org)).

The work hardening rate along with excellent elongation combine to give DP steels much higher ultimate tensile strength than conventional steels of similar yield

strength. Figure 2.5 where the quasi-static stress-strain behavior of high-strength, low alloys (HSLA) steel is compared with DP steel. It indicates, the DP steel yield stress and yield point are deferent although the gradient of elastic is seemed similar.

The DP steel exhibits higher initial work hardening rate, uniform and total elongation, ultimate tensile strength, and lower YS/TS ratio than the similar yield strength HSLA. DP and other AHSS also have another important benefit compared with conventional steels. The bake hardening effect, which increase in yield strength resulting from prestraining (representing the work hardening due to stamping or other manufacturing processes) and elevated temperature aging (representing the curing temperature of paint bake ovens) continues to increase with increasing strain.

Conventional baked hardening effects, of BH steels, for example, remain somewhat constant after prestrains of about 2%. The extent of the bake hardening effect in AHSS depends on the specific chemistry and thermal histories of the steels. DP steels is designed to provide ultimate tensile strengths of up to 1000 MPa (<http://www.autosteel.org>).

### **2.3 Sheet Metal Forming**

Sheet metal forming (SMF) is one of the most common metal manufacturing processes used. Sheet metal forming is more focused on the plastic deformation principle.

Compared to casting and machining, sheet-metal parts offer the advantages of light weight and versatile shape. The technical-economic advantages of SMF are that it is a highly efficient process that can be used to produce complex parts. It can produce parts with the high degree of dimensional accuracy and increased mechanical properties along with a good surface finish. But the limitation is that the deformation imposed in SMF process is complicated (Crisbon D. J, 2003).

### 2.3.1 Sheet Metal Forming Process

Sheet metal forming process is a grouping of many complementary processes that are used to form sheet metal parts. One or more of these processes is used to take a flat sheet of ductile metal, and mechanically apply deformation forces that altered the shape of the material. Before deciding on the processes, one should determine whether a particular sheet metal can be formed into the desired shape without failure. Table 2.1 describes briefly the characteristic of sheet metal forming processes.

The characteristics of sheet metal forming process are :

- the work piece is a sheet or a part fabricated from a sheet.
- the surfaces of the deforming material and of the tools are in contact.
- the deformation usually causes significant changes in shape, but not in cross-section (sheet thickness and surface characteristics) of the sheet. In some cases, the magnitude of permanent plastic and recoverable elastic deformation is comparable, therefore springback may be significant.

Table 2.1: The Characteristic of Sheet Metal forming Processes

Processes	Characteristics
Roll forming	<ul style="list-style-type: none"> <li>• long parts with constant complex cross-sections;</li> <li>• good surface finish;</li> <li>• high production rates;</li> <li>• high tooling costs.</li> </ul>
Stretch forming	<ul style="list-style-type: none"> <li>• long parts with constant complex cross-sections;</li> <li>• good surface finish;</li> <li>• high production rates;</li> <li>• high tooling costs.</li> </ul>
Drawing	<ul style="list-style-type: none"> <li>• shallow or deep parts with relatively simple shapes;</li> <li>• high production rates;</li> <li>• high tooling and equipment costs.</li> </ul>
Stamping	<ul style="list-style-type: none"> <li>• includes a variety of operations, such as punching, embossing, bending, flanging, and</li> </ul>

	coining; <ul style="list-style-type: none"> <li>• simple or complex shapes formed at high production rates;</li> <li>• tooling and equipment costs can be high, but labor cost is low.</li> </ul>
Rubber forming	<ul style="list-style-type: none"> <li>• drawing and embossing of simple or complex shapes;</li> <li>• sheet surface protected by rubber membranes;</li> <li>• flexibility of operation;</li> <li>• low tooling costs.</li> </ul>
Spinning	<ul style="list-style-type: none"> <li>• small or large axisymmetric parts;</li> <li>• good surface finish; low tooling costs, but labor costs can be high unless operations are automated.</li> </ul>
Superplastic forming	<ul style="list-style-type: none"> <li>• complex shapes, fine detail and close tolerances;</li> <li>• forming times are long, hence production rates are low;</li> <li>• parts not suitable for high-temperature use.</li> </ul>
Peen forming	<ul style="list-style-type: none"> <li>• shallow contours on large sheets;</li> <li>• flexibility of operation;</li> <li>• equipment costs can be high;</li> <li>• process is also used for straightening parts.</li> </ul>
Explosive forming	<ul style="list-style-type: none"> <li>• very large sheets with relatively complex shapes, although usually axisymmetric;</li> <li>• low tooling costs, but high labor cost;</li> <li>• suitable for low-quantity production;</li> <li>• long cycle times.</li> </ul>
Magnetic-pulse forming	<ul style="list-style-type: none"> <li>• shallow forming, bulging, and embossing operations on relatively low-strength sheets;</li> <li>• most suitable for tubular shapes;</li> <li>• high production rates;</li> <li>• requires special tooling.</li> </ul>

Stamping is one type of sheet metal forming process. Generally, the deformation of sheet materials in the stamping process is classified by four types of deformation modes; i.e bending, deep drawing, stretching and stretching flanging. Since this project deals with the bending process, this study will be focused on the bending operation.

Bending is the plastic deformation of metals about a linear axis called the bending axis with little or no change in the surface area. It is not only to form pieces such as L, U, or V profile but also to improve the stiffness of a piece by increasing its moment of inertia. Bending involved springback phenomenon. This happened when during the unloading process. The centre region of sheet remains elastic and so on unloading elastic recovery occurs.

## **2.4 Springback**

Springback is the elastically-driven change in shape of a part upon unloading after forming, is a growing concern as manufacturers increasingly rely on materials with higher strength-to-modulus ratios than the traditional low strength steel according to Firat M (2007). Effect of springback is by changing the shape and dimension which is create major problem in the assembly.

There are two terms that are important in springback namely; springback controlling during forming and springback prediction in die design stage. Springback may not be categorized as a defect. However this geometrical discrepancy can cause ill-fitting in part assembly and geometric deviation of the intended design. If springback could be predicted, the tool and die could be accurately designed and built. There are many factors could affect springback in the process, such as material variation in mechanical properties, sheet thickness, tooling geometry, processing parameters and lubricant condition (Boljvonik V., 2004).

### **2.4.1 Basic Theory of Springback**

Basically, in springback the deformation is caused by elastic recovery. As a consequence, changes occur in the dimensions of the plastic-deformed workpiece upon removing the load. Equation (2.1) from Hosford W.F and Robert M.C (1993) explained



that the permanent deformation ( $\varepsilon_p$ ) is expressed as the difference between the plastic ( $\varepsilon_{pl}$ ) and the elastic ( $\varepsilon_e$ ) formation.

$$\varepsilon_{pl} = \varepsilon_{total} - \varepsilon_e \quad (2.1)$$

While a workpiece is loaded, it will have bend radius ( $R_i$ ), bend angle ( $\varphi_i = 180^\circ - \alpha_1$ ) and profile angle ( $\alpha_1$ ) as the characteristic dimensions consequence to plastic deformation, Figure 2.6.

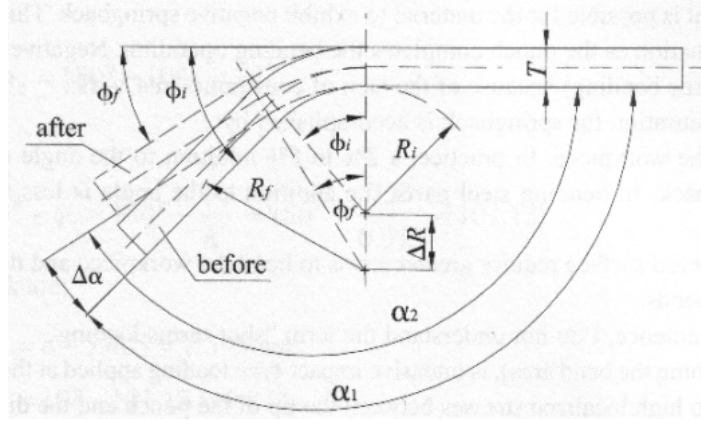


Figure 2.6: Schematic illustration of springback (Hosford W.F and Robert M.C,1993)

The final work pieces after being unloaded are bending radius ( $R_f$ ), bend angle ( $\varphi_f = 180^\circ - \alpha_2$ ) and profile angle, ( $\alpha_2$ ). The final angle after springback is smaller ( $\varphi_f < \varphi_i$ ) and the final bend radius is larger ( $R_f > R_i$ ) than before. There are two ways to understand and compensate for springback. One is to obtain or develop a predictive model of the amount of springback (which has been proven experimentally). The other way is to define a quantity to describe the amount of springback. A quantity characterizing springback is the springback factor ( $K_s$ ) depends only on the R/T ratio, R (radius) and T (thickness), which is determined as Equation (2.2) (Hosford W.F and Robert M.C, 1993).

$$K_s = \frac{R_i + \frac{T}{2}}{R_f + \frac{T}{2}} = \frac{\frac{2R_i}{T} + 1}{\frac{2R_f}{T} + 1} = \frac{\varphi_f}{\varphi_i} = \frac{180^\circ - \alpha_2}{180^\circ - \alpha_1} \quad (2.2)$$

According to Hosford W.F and Robert M.C (1993), there are two conditions that happen during sheet metal bending, which are tensile and compression. The moment,  $M$  that produced this bend calculated by assumes that there is no net external force in the  $x$  direction ( $\sum F_x = 0$ ). The internal force,  $dF_x$  have to be considered. The relation the internal force indicates as Equation (2.3).

$$dF_x = \sigma_x w dz \quad (2.3)$$

Where  $\sigma_x$  is the stress,  $w$  is width and  $dz$  is a portion of considered thickness. The change in bending moment,  $\Delta M$  as Equation (2.4)

$$\Delta M = 2w \int_0^{t/2} \Delta \sigma_x z dz = 2w \int_0^{t/2} E' \left( \frac{1}{r} - \frac{t}{r'} \right) z^2 dz = \frac{wE'}{12} \left( \frac{1}{r} - \frac{1}{r'} \right) \quad (2.4)$$

Where,  $E'$  is plane strain modulus,  $\Delta \sigma_x$  is unloading elastic. If the tensile yield stress is  $Y$ , the flow stress in plane strain will be  $\sigma_0 = \sqrt{4/3} Y$  For the ideally plastic  $\sigma_x = \sigma_0$ . The elastic unloading after removal of the loads results in the residual stresses presented in Figure 2.7.

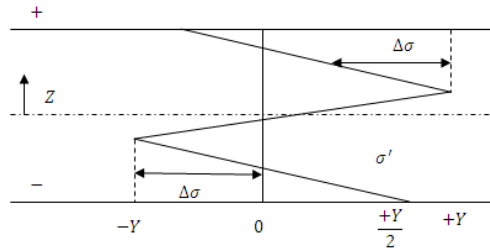


Figure 2.7: The elastic unloading after removal of the loads results in the residual stresses. (Hosford W.F and Robert M.C,1993)

Notes that for outer surface

$$z = t/2$$

Compressive residual stress

$$\sigma'_x = -\sigma_0/2$$

For inside surface

$$z = -t/2$$

Tensile strength

$$\sigma'_x = +\sigma_0/2$$

While for work hardening material, if exponential based plasticity is used where k is strength coefficient value

$$\bar{\sigma} = k\bar{\epsilon}^n = k' \left( \frac{z}{r} \right)^n. \quad (2.5)$$

Where

$$k' = k \left( \frac{4}{3} \right)^{\frac{n+1}{2}}$$

From Equation (2.5) substituting  $\sigma_x$ , the equation become

$$M = \left( \frac{2}{2+n} \right) \frac{wk'}{r^n} \left( \frac{t}{2} \right)^{2+n} \quad (2.6)$$

After the springback,  $-\Delta M = 0$

$$\left( \frac{1}{r} - \frac{1}{r'} \right) = \left( \frac{6}{2+n} \right) \left( \frac{k'}{E'} \right) \left( \frac{t}{2r} \right)^n \left( \frac{1}{t} \right) \quad (2.7)$$

The variation of  $\sigma_x$ ,  $\Delta\sigma_x$  and  $\sigma'_x$  refer to Figure 2.8 which shows the stress distribution under bending moment and after unloading for work-hardening material.

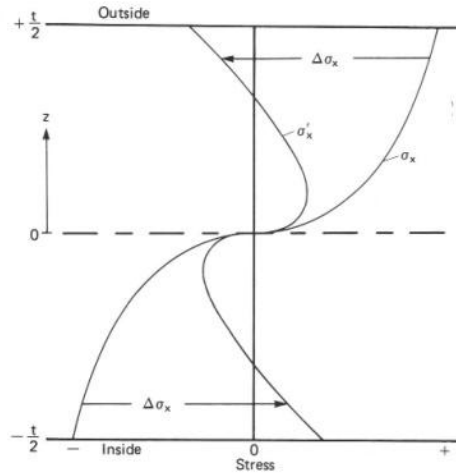


Figure 2.8: The stress distribution under bending moment and after unloading for work-hardening material. (Hosford W.F and Robert M.C,1993)

Residual stress can be determined using Equation (2.8).

$$\sigma'_x = k' \left( \frac{z}{r} \right)^n \left[ 1 - \left( \frac{3}{2+n} \right) \left( \frac{2z}{t} \right)^{1-n} \right] \quad (2.8)$$

The magnitude springback prediction can be defined using either Equation (2.7) or (2.9)

$$\frac{1}{r} - \frac{1}{r'} = \frac{3\sigma_0}{tE'} \quad (2.9)$$

The basic theory of prediction springback above is only for 1D formulation. For 3D cases, the FEA approach should be used to consider each of the axes involved.

### 2.4.2 Springback Prediction Techniques

Various experimental technique and procedures have been developed to study springback. The most commonly used techniques are U-bending, V-bending, cylindrical bending and flanging. These methods served large level of springback and can be easily measured. Usually by these techniques, the basic parameters such as  $R/t$  ratio (tool radius to sheet thickness), geometric parameters of the tools, mechanical properties of sheet material and the friction parameters are studied. The major drawback of these experiments is that they cannot imitate process conditions that take place during sheet metal forming.

Referred to Carlos G et.al, (2004), in order to obtain a better understanding of springback deformation in high strength anisotropic steels a combined numerical and experimental investigation was performed in the current work. A standard U-shaped geometry was selected for the experimental and numerical analyses. Experiments were carried out using a specially designed stamping apparatus and the explicit to implicit sequential solution technique was utilized in the numerical simulations. Based on the experimental and numerical results, significant insight was obtained for high strength anisotropic steels that can increase their industrial viability.

The U-shaped cross-sections presented in NUMISHEET'93 (Figure 2.9) was selected for this study, because it is a benchmark problem for isotropic springback analyses. For the U-shaped geometry there is a standard method to measure springback. Figure 2.10 shows details of the actual geometry investigated in the experimental and numerical analyses, and the variables that will be used to measure springback.

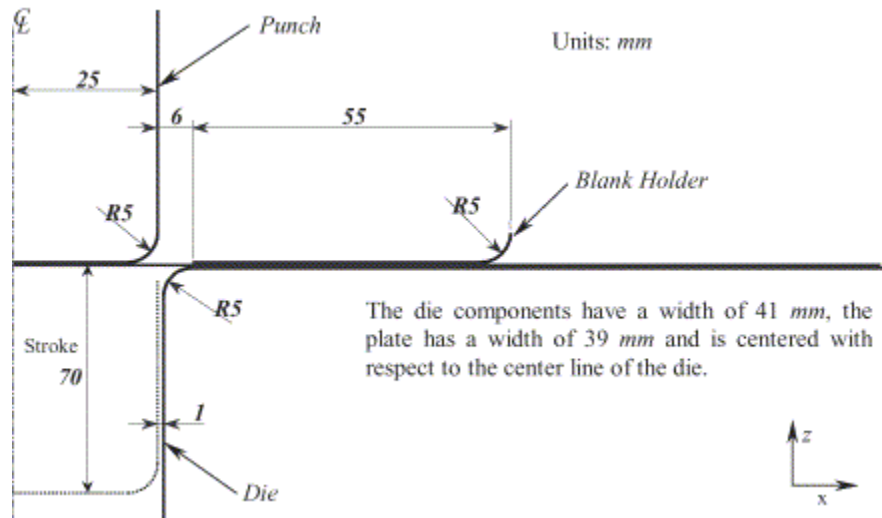


Figure 2.9: Details of NUMISHEET'93 benchmark. (Carlos G., et.al, 2004)

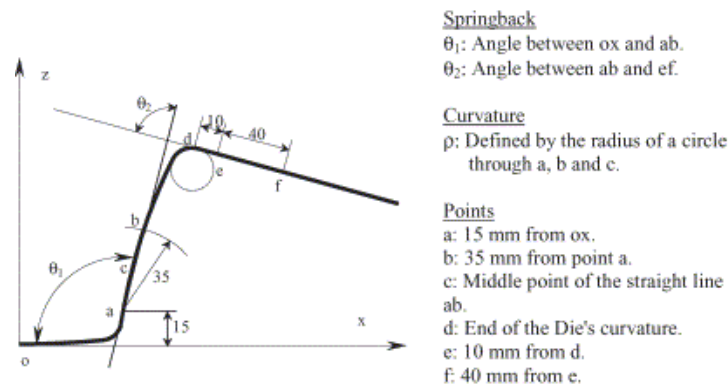


Figure 2.10: Measurement parameters for springback. (Carlos G., et.al, 2004)

## 2.5 Finite Element Analysis

Numerical simulation was used in finite element method prior tool to prevent the undesirable effects of materials technological processing. This method is not only capable to lowering the cost and shortening delivery periods, but also supporting in achieving the higher quality.

The use of finite element analysis is beneficial in the design of tooling in sheet metal forming operation because it is more cost effective than trial and error. The

purpose of analysis is to assist the design by predicting the material deformation, including the forces and stresses necessary to execute the forming operation.

Finite Element method is a method to find the solution of the continue structure. The continue structure is divided into small elements that are discrete. Then the elements are considered to apply a functional approach to a particular variable. The continue structure may occur in solid, liquid or gas form. In the application of metal forming processes, the continue structure of material is the metal which are including the mechanism of variable.

According to Haryanti.S (2007), first introduction to of the finite element was determined by Clough in 1960. Before that, the idea of it has been expanded by Greenstadt in 1959. The approaches base on cell, not the point of the continue structure. Basically, he divided the solution into a row of interconnected sub cell. Where, he applied a discrete function of every cell and an interpolation function which is used for continuity in the entire cell.

Plastic deformation was introduced at the end of 1970, in which nonlinear analysis be adopted. Start with the implement of the membrane elements in the formulation of elastic-plastic material. Around 1980, study of the membrane identified inadequate to show sheet metal behavior. Then the shell element is applied, and focuses on applications and modeling techniques rather than the mathematical approach.

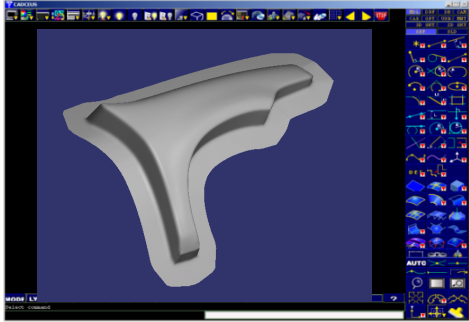
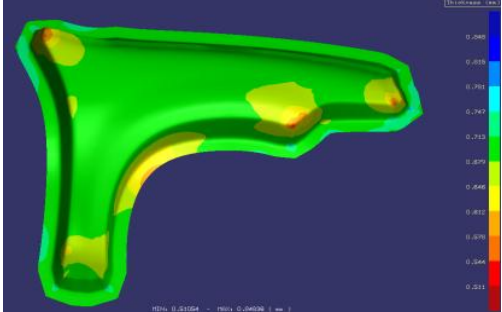
In modeling of metal forming, there are two important things have to be considered, which is the dynamic factor and non linearity (plasticity). The dynamic factor for the formation of the metallic material involves the flow of material and movement of the tool. While non linear factor caused by the deformation of plastic, which does not comply with Hooke Law. Recently, the FEM became a standard procedure in metal forming industries, particularly during the planning and product development.

### **2.5.1 Application of FEM in Metal Forming**

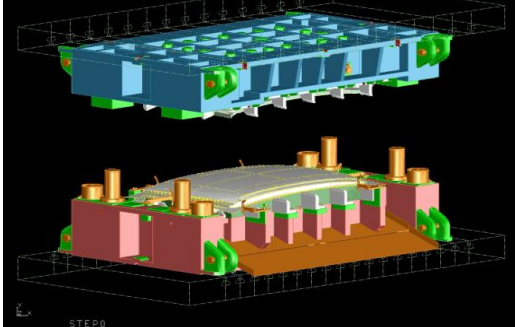
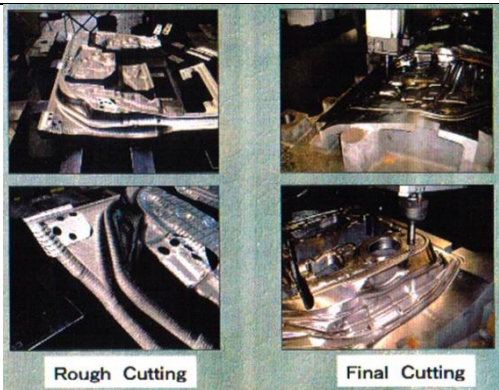

The application of metal forming including FEM analysis described metal forming theory and how experimental techniques can be used to study metal forming operations

with great accuracy. For each processes such as sheet-metal forming, it explained how finite element analysis (FEA) can be applied with great precision to characterize the forming conditions and optimized the processes. FEA has made it possible to build realistic FEM models of most metal forming processes, including complex three-dimensional forming operations. Thus, using FEA, it is now possible to visualize any metal forming process and to study strain, stress, and other forming conditions inside the parts being manufactured as they develop throughout the process. Applied metal forming included FEM consists of five basic steps, which are described in Table 2.2 below (source of figure from LS-DYNA Users Manual, 2001).

Table 2.2: Basic steps of FEM application in metal forming.

Steps of FEM application in metal forming	Illustration
<p>Concept Product Design</p> <ul style="list-style-type: none"> <li>- Geometry part import to software. (pre-processor).</li> <li>- The model is constructed using software.</li> </ul>	
<p>Analysis</p> <ul style="list-style-type: none"> <li>- Analysis done by solver.</li> <li>- Result creates counter, deformation, FLD, stress plot etc.</li> <li>- Result will be reviewed and studied.</li> </ul>	



<p>Die Design in 3D</p> <ul style="list-style-type: none"> <li>- Tooling design step according to product FEA.</li> </ul>	
<p>Manufacturing processes</p> <ul style="list-style-type: none"> <li>- Tooling construction and manufacturing.</li> </ul>	
<p>End Product</p>	

### 2.5.2 Finite Element Software

Previously, the software for simulating forming operations such as stamping required expensive, high-end dedicated workstations and highly trained personnel intimately familiar with the in and out of finite-element analysis (FEA). Even then, metalformers could not be sure that the coding behind such software would accurately predict real-

## REFERENCE

- Akhtar S. K. and Huang S. (1995). *Continuum Theory of Plasticity*. John Wiley & Sons.
- Boljavonic V. (2004). Sheet Metal Forming Processes and Die Design .Industrial Press, p64-67
- Burchitz I. (2005)., *Springback Improvement of its Predictability*, Literature Study Report, Netherland Institute for Metals Research,
- Cao J., Liu Z.H and Liu W.K (1999). *Prediction of Springback in Straight Flanging Operation*. Submitted to Symposium Advances in Sheet Metal Forming. IMECE '99
- Crisbon D. J (2003), *Experimental Measurement and Finite Element Simulation of Springback in stamping Aluminium Alloy Sheet for Auto-Body Panel Application*, Master of Science Thesis, Department of Mechanical Engineering , Mississippi State University Science.
- Cristopher P. G. (2004)., *Springback of Simple Mechanical Test Specimen: Comparison between theory and finite elemnt predictions obtained using LS-DyNA and Dynaform*, PHD of Eng. Thesis, Metal Forming Analysis Corporation, Kingston, Ontario, Canada
- Firat M. (2007), *U-channel forming analysis with an emphasis on springback deformation*, *Journal of Material and Design, Elsevier*. 28 (2007) 147-154.
- Fionn D. and Nik P. (2004), *Introduction to Computational Plasticity*. Oxford University Press, p11-180.

Gan W., Babu S.S., Kapustka N. and Robert H. Wagoner (2006), Microstructure Effects on the Springback of Advanced High-Strength Steel , *Journal Of Metallurgical and Materials Transactions A*, Volume 37, Number 11 / November, 2006

Haryanti S. (2007) *Explicit and Implicit Time Integration in the Finite Element Modeling of Metal Forming Process*, Journal Ilmiah Mesin Universitas Trisakti Vol. 9, No. 4, September 2007

Hosford W. F. and Robert M.C.(1993), *Metal forming-mechanics and metallurgy*. Prentice Hall, p1-65, p270-280, p286-304, p327-340, p351-354.

Jeswiet J. J. , M. Geiger , U. Engel , M. Kleiner , M. Schikorra , J. Duflou , R.Neugebauer P. Bariani and S. Bruschi (2008). *Metal Forming Progress Since 2000*. CIRP Journal of Manufacturing Science and Technology 1 (2008) 2–17.

Kenneth G. B and Michael K.B (1999), *Engineering Material, Properties and Selection (6<sup>th</sup> ed)*. Prentice Hall, p354-407.

Li K.P, Carden W.P and Wagoner R.H (2002), Simulation of Springback. *International Journal of Mechanical Science*, 44(1):103-122.

Liu Y.C (1984), *Springback Reduction in U-channel: Double Bend Technique*. Journal of Applied Metalworking. Vol. 3, pg 148-156

LS-DYNA Keyword Users Manual version 960,Livermore Software Technology Corporation, 2001

Marciniak Z, Duncan J.L and Hu S.J,(2002), *Mechanics of Sheet Metal Forming*. Butterworth Heinemann, p1-13, p14-27, p30-43.

Mohd Nizam K (2008), *Optimising Deep Drawing Process Parameter using FE simulation* . Master of Mechanical Engineering Thesis, Department of

Mechanical and Manufacturing Engineering , Universiti Tun Hussien Onn Malaysia .

Monfort G., And Bragard A. (1985). *A Simple Model of Shape Errors in Forming and its Application to the Reduction of Springback*. Springer Link Journal of Applied Metalworking (1986) Volume 4, Number 3 / July, pg 283-291

Song N., Qian D., Jian C, Wing K.L and Shaofan L. (2004). *Effective Models for Prediction of Springback in Flanging*. ASME Journal of Engineering Materials and Technology (2004) Volume 123, Issue 4, 456

Xiaoding Z., Zhaohui M. and Li W. (2007). *Current Status of Advanced High Strength Steel for Auto-making and its Development in Baosteel*. Baosteel Research Institute, Shanghai 201900, China

INTERNATIONAL IRON & STEEL INSTITUTE (2006). “Advanced High Strength Steel Application Guidelines”. Version 3.

Material Data Sheet of Dual Phase Steel (2005)

[http://www.salzgitterflachstahl.de/.../Material\\_data\\_sheets/Dual\\_phase\\_steel\\_Material\\_data\\_sheet\\_11\\_111\\_edition\\_09\\_05](http://www.salzgitterflachstahl.de/.../Material_data_sheets/Dual_phase_steel_Material_data_sheet_11_111_edition_09_05)

<http://www.keytometals.com>

<http://www.autosteel.org>

<http://www.steel.org>

<http://www.ssab.com>